

Measurements of the Cross Section for $e^+e^- \rightarrow$ hadrons at Center-of-Mass Energies from 2 to 5 GeV

J. Z. Bai¹, Y. Ban¹⁰, J. G. Bian¹, A. D. Chen¹, H. F. Chen¹⁶, H. S. Chen¹, J. C. Chen¹, X. D. Chen¹, Y. B. Chen¹, B. S. Cheng¹, S. P. Chi¹, Y. P. Chu¹, J. B. Choi³, X. Z. Cui¹, Y. S. Dai¹⁹, L. Y. Dong¹, Z. Z. Du¹, W. Dunwoodie¹⁴, H. Y. Fu¹, L. P. Fu⁷, C. S. Gao¹, S. D. Gu¹, Y. N. Guo¹, Z. J. Guo², S. W. Han¹, Y. Han¹, F. A. Harris¹⁵, J. He¹, J. T. He¹, K. L. He¹, M. He¹¹, X. He¹, T. Hong¹, Y. K. Heng¹, G. Y. Hu¹, H. M. Hu¹, Q. H. Hu¹, T. Hu¹, G. S. Huang², X. P. Huang¹, Y. Z. Huang¹, J. M. Izen¹⁷, X. B. Ji¹¹, C. H. Jiang¹, Y. Jin¹, B. D. Jones¹⁷, J. S. Kang⁸, Z. J. Ke¹, H. J. Kim¹³, S. K. Kim¹³, T. Y. Kim¹³, D. Kong¹⁵, Y. F. Lai¹, D. Li¹, H. B. Li¹, H. H. Li⁶, J. Li¹, J. C. Li¹, P. Q. Li¹, Q. J. Li¹, R. Y. Li¹, W. Li¹, W. G. Li¹, X. N. Li¹, X. Q. Li⁹, B. Liu¹, F. Liu⁶, Feng Liu¹, H. M. Liu¹, J. Liu¹, J. P. Liu¹⁸, T. R. Liu¹, R. G. Liu¹, Y. Liu¹, Z. X. Liu¹, X. C. Lou¹⁷, G. R. Lu⁵, F. Lu¹, J. G. Lu¹, Z. J. Lu¹, X. L. Luo¹, E. C. Ma¹, J. M. Ma¹, R. Malchow⁴, H. S. Mao¹, Z. P. Mao¹, X. C. Meng¹, X. H. Mo¹, J. Nie¹, Z. D. Nie¹, S. L. Olsen¹⁵, D. Paluselli¹⁵, H. Park⁸, N. D. Qi¹, X. R. Qi¹, C. D. Qian¹², J. F. Qiu¹, Y. K. Que¹, G. Rong¹, Y. Y. Shao¹, B. W. Shen¹, D. L. Shen¹, H. Shen¹, X. Y. Shen¹, H. Y. Sheng¹, F. Shi¹, H. Z. Shi¹, X. F. Song¹, J. Y. Suh⁸, H. S. Sun¹, L. F. Sun¹, Y. Z. Sun¹, S. Q. Tang¹, W. Toki⁴, G. L. Tong¹, G. S. Varner¹⁵, J. Wang¹, J. Z. Wang¹, L. Wang¹, L. S. Wang¹, P. Wang¹, P. L. Wang¹, S. M. Wang¹, Y. Y. Wang¹, Z. Y. Wang¹, C. L. Wei¹, N. Wu¹, D. M. Xi¹, X. M. Xia¹, X. X. Xie¹, G. F. Xu¹, Y. Xu¹, S. T. Xue¹, W. B. Yan¹, W. G. Yan¹, C. M. Yang¹, C. Y. Yang¹, G. A. Yang¹, H. X. Yang¹, W. Yang⁴, X. F. Yang¹, M. H. Ye², S. W. Ye¹⁶, Y. X. Ye¹⁶, C. S. Yu¹, C. X. Yu¹, G. W. Yu¹, Y. Yuan¹, B. Y. Zhang¹, C. Zhang¹, C. C. Zhang¹, D. H. Zhang¹, H. L. Zhang¹, H. Y. Zhang¹, J. Zhang¹, J. W. Zhang¹, L. Zhang¹, L. S. Zhang¹, P. Zhang¹, Q. J. Zhang¹, S. Q. Zhang¹, X. Y. Zhang¹¹, Y. Y. Zhang¹, Z. P. Zhang¹⁶, D. X. Zhao¹, H. W. Zhao¹, Jiawei Zhao¹⁶, J. W. Zhao¹, M. Zhao¹, P. P. Zhao¹, W. R. Zhao¹, Y. B. Zhao¹, Z. G. Zhao¹, J. P. Zheng¹, L. S. Zheng¹, Z. P. Zheng¹, B. Q. Zhou¹, G. M. Zhou¹, L. Zhou¹, K. J. Zhu¹, Q. M. Zhu¹, Y. C. Zhu¹, Y. S. Zhu¹, Z. A. Zhu¹, B. A. Zhuang¹, and B. S. Zou¹.

(BES Collaboration)

¹ *Institute of High Energy Physics, Beijing 100039, People's Republic of China*

² *China Center of Advanced Science and Technology, Beijing 100080, People's Republic of China*

³ *Chonbuk National University, Chonju 561-756, Korea*

⁴ *Colorado State University, Fort Collins, Colorado 80523*

⁵ *Henan Normal University, Xinxiang 453002, People's Republic of China*

⁶ *Huazhong Normal University, Wuhan 430079, People's Republic of China*

⁷ *Hunan University, Changsha 410082, People's Republic of China*

⁸ *Korea University, Seoul 136-701, Korea*

⁹ *Nankai University, Tianjin 300071, People's Republic of China*

¹⁰ *Peking University, Beijing 100871, People's Republic of China*

¹¹ *Shandong University, Jinan 250100, People's Republic of China*

¹² *Shanghai Jiaotong University, Shanghai 200030, People's Republic of China*

¹³ *Seoul National University, Seoul 151-742, Korea*

¹⁴ *Stanford Linear Accelerator Center, Stanford, California 94309*

¹⁵ *University of Hawaii, Honolulu, Hawaii 96822*

¹⁶ *University of Science and Technology of China, Hefei 230026, People's Republic of China*

¹⁷ *University of Texas at Dallas, Richardson, Texas 75083-0688*

¹⁸ *Wuhan University, Wuhan 430072, People's Republic of China*

¹⁹ *Zhejiang University, Hangzhou 310028, People's Republic of China*

(February 9, 2001)

The QED running coupling constant evaluated at the Z pole, $\alpha(M_Z^2)$, and the anomalous magnetic moment of the muon, $a_\mu = (g - 2)/2$, are two fundamental quantities that are used to test the Standard Model (SM) [1]. Among the three input parameters generally used in global fits to electroweak data, $\alpha(M_Z^2)$ has the largest experimental uncertainty and is the primary limit on the precision of SM calculations of the mass of the Higgs particle. The value of a_μ is of interest because of its sensitivity to large energy scales and very high order radiative corrections. Any deviation between the SM predicted value for a_μ^{SM} and its experimentally measured value, a_μ^{Exp} , would be an indication of new physics. The dominant uncertainties in both $\alpha(M_Z^2)$ and a_μ^{SM} are due to the effects of hadronic vacuum polarization, which cannot be reliably calculated. Instead, with the application of dispersion relations, experimentally measured R values are used to determine the vacuum polarization [1], where R is the lowest order cross section for $e^+e^- \rightarrow \gamma^* \rightarrow \text{hadrons}$ in units of the lowest-order QED cross section for $e^+e^- \rightarrow \mu^+\mu^-$, namely $R = \sigma(e^+e^- \rightarrow \text{hadrons})/\sigma(e^+e^- \rightarrow \mu^+\mu^-)$, where $\sigma(e^+e^- \rightarrow \mu^+\mu^-) = \sigma_{\mu\mu}^0 = 4\pi\alpha^2(0)/3s$.

The uncertainties in $\alpha(M_Z^2)$ and a_μ^{SM} are dominated by the errors in the values of R in the center of mass (cm) energy range below 5 GeV. These were measured about 20 years ago with a precision of about 15 ~ 20%. Thus, new measurements of R in the energy region between 2 and 5 GeV with significantly improved precision are very important [1]. In this paper, we report measurements of R at 85 cm energies between 2 and 5 GeV, with an average precision of 6.6%.

The measurements were carried out using the upgraded Beijing Spectrometer (BESII) at the Beijing Electron Positron Collider (BEPC). Currently BEPC is the only e^+e^- machine operating in the 2 to 5 GeV cm energy region; its peak luminosity at the J/ψ resonance is about $5 \times 10^{30}/\text{cm}^2 \cdot \text{s}$. BESII is a conventional collider detector based on a large solenoid magnet with a central field of 0.4 T. It is described in detail in Ref. 2.

A vertex chamber (VC) comprising 12 tracking layers surrounds a beryllium beampipe. This provides input to the trigger system, as well as coordinate information that improves the momentum resolution for charged tracks. The primary tracking device is the cylindrical main drift chamber (MDC). This has 40 layers of sense wires and yields precise measurements of charged particle trajectories; it also provides dE/dx information which is used for charged particle identification. Outside the MDC, there is a barrel time-of-flight system (BTOF) consisting

of an array of 48 plastic scintillator counters read out at each end by fine-mesh photomultiplier tubes located inside the magnetic field volume. Electron and photon showers are detected in a sampling-type barrel shower counter (BSC) that covers 80 % of the total solid angle. This consists of 24 layers of self-quenching streamer tubes interspersed with lead; each layer has 560 tubes. The outermost component of BESII is a muon identification system consisting of three double layers of proportional tubes interspersed in the iron flux return of the magnet. Table I lists the values of the main parameters which describe the performance of the BES detector.

TABLE I. Major parameters describing the performance of the BESII spectrometer.

Detector	Major parameter	BESII
VC	$\sigma_{xy}(\mu\text{m})$	100
	$\sigma_{xy}(\mu\text{m})$	190-220
MDC	$\Delta p/p$ (%)	$1.78\sqrt{1+p^2}$
	$\sigma_{dE/dx}$ (%)	8.4
BTOF	σ_T (ps)	180
BSC	$\Delta E/\sqrt{E}$ (%)	23
	σ_z (cm)	2.3
μ counter	σ_z (cm)	5.5

Following a preliminary scan that measured R at six energy points between 2.6 and 5 GeV [3], we performed a finer R scan with 85 energy points covering the energy region between 2 and 4.8 GeV [4]. In order to understand beam-associated backgrounds, separated beam data were accumulated at 24 different energies and single beam runs for both e^- and e^+ were done at 7 energies interspersed throughout the entire energy range. Special runs were taken at the J/ψ resonance to determine the trigger efficiency. The J/ψ and $\psi(2S)$ resonances were scanned at the beginning and end of the R scan to calibrate the cm energy.

Experimentally, the value of R is determined from the number of observed hadronic events, N_{had}^{obs} , by the relation

$$R = \frac{N_{had}^{obs} - N_{bg} - \sum_l N_{ll} - N_{\gamma\gamma}}{\sigma_{\mu\mu}^0 \cdot L \cdot \epsilon_{had} \cdot \epsilon_{trg} \cdot (1 + \delta)}, \quad (1)$$

where N_{bg} is the number of beam-associated background events; $\sum_l N_{ll}$, ($l = e, \mu, \tau$) are the numbers of lepton-pair events from one-photon processes and $N_{\gamma\gamma}$ the number of two-photon process events that are misidentified as hadronic events; L is the integrated luminosity; δ is the radiative correction; ϵ_{had} is the detection efficiency for hadronic events; and ϵ_{trg} is the trigger efficiency.

The triggers were the same as those used in our previous R scan [3]. The trigger efficiencies, measured by comparing the responses to different trigger requirements in special runs taken at the J/ψ resonance, are determined to be 99.96%, 99.33% and 99.76% for Bhabha, dimuon and hadronic events, respectively. The errors in the trigger efficiencies for Bhabha, dimuon and hadronic events are 0.5%.

We developed a set of requirements on fiducial regions, vertex positions, track fit quality, maximum and minimum BSC energy deposition, track momenta and time-of-flight hits that preferentially distinguish one-photon multi-hadron production from all possible contamination mechanisms. Residual background contributions are due to cosmic rays, lepton pair production, two-photon interactions and single-beam-related processes. Additional requirements are imposed on two-prong events, for which cosmic ray and lepton pair backgrounds are especially severe [3].

An acceptable charged track must be in the polar angle region $|\cos(\theta)| < 0.84$, have a good helix fit, and not be clearly identified as an electron or muon. The distance of closest approach to the beam axis must be less than 2 cm in the transverse plane, and must occur at a point for which $|z| < 18$ cm. In addition, the following criteria must be satisfied: (i) $p < p_{beam} + 5 \times \sigma_p$, where p and p_{beam} are the track and incident beam momenta, respectively, and σ_p is the momentum uncertainty for a charged track for which $p = p_{beam}$; (ii) $E < 0.6E_{beam}$, where E is the BSC energy associated with the track, and E_{beam} is the beam energy; (iii) $2 < t < t_p + 5 \times \sigma_t$ (in ns.), where t is the measured time-of-flight for the track, and t_p is the time-of-flight calculated assigning the proton mass to the track; σ_t is the resolution of the BTOF system.

After track selection, event selection requires the presence of at least two charged tracks, of which at least one satisfies all of the criteria listed above. In addition, the total energy deposited in the BSC must be greater than $0.28E_{beam}$, and the selected tracks must not all point into the forward ($\cos\theta > 0$) or the backward ($\cos\theta < 0$) hemisphere.

For two-prong events, residual cosmic ray and lepton pair background is removed by requiring that the tracks not be back-to-back, and that there be at least two isolated energy clusters in the BSC with $E > 100$ MeV that are at least 15° in azimuth from the closest charged track. This last requirement rejects radiative Bhabha events.

These requirements eliminate virtually all cosmic rays and most of the lepton pair events. The remaining background contributions due to lepton pairs (N_{ll}) and two-photon events ($N_{\gamma\gamma}$) are estimated from Monte Carlo simulation and subtracted as indicated in Eq. (1).

The number of hadronic events and the beam-associated background level are determined by fitting the distribution of event vertices along the beam direction with a Gaussian for real hadronic events and a poly-

nomial of degree two for the background, as shown in Fig. 1.

The beam-associated backgrounds can also be subtracted by applying the same hadronic event selection criteria to separated-beam data. The number of separated-beam events, N_{sep} , surviving these criteria is obtained. The number of beam-associated background events, N_{bg} , in the corresponding hadronic event sample is given by $N_{bg} = f \times N_{sep}$, where f is the ratio of the products of the pressure at the collision region and the integrated beam current for colliding- and separated-beam runs. The differences between R values obtained using these two methods to determine the beam-associated background range between 0.3 and 2.3%, depending on the energy. These differences are included in the systematic uncertainty.

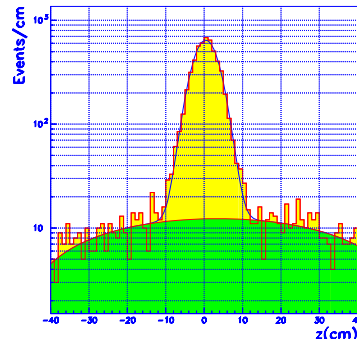


FIG. 1. The primary vertex distribution on the beam (z) axis for the hadronic event sample selected at a cm energy of 2.6 GeV [1999 data].

The integrated luminosity is determined from the number of large-angle Bhabha events selected using only the BSC energy deposition. We require two BSC energy clusters, the one with the larger deposited energy being in the polar angle region $|\cos(\theta)| < 0.70$. In addition, each cluster must have energy $> 1.0 \text{ GeV} \times (E_{cm}/3.55 \text{ GeV})$, and the pair must satisfy $2^\circ < ||\phi_1 - \phi_2| - 180^\circ| < 16^\circ$, where ϕ_1 and ϕ_2 are the respective azimuthal angles. The $\Delta\phi > 2^\circ$ requirement separates $e^+e^- \rightarrow e^+e^-$ events, which are not exactly back-to-back because of the magnetic field, from $e^+e^- \rightarrow \gamma\gamma$ events.

JETSET, the Monte Carlo event generator that is commonly used to simulate $e^+e^- \rightarrow$ hadrons, was not intended to be applicable to the low energy region, especially that below 3 GeV. A special joint effort was made by the Lund group and the BES collaboration to develop the LUARLW generator, which uses a formalism based on the Lund Model Area Law, but without the extreme-high-energy approximations used in JETSET's string fragmentation algorithm [5]. The final states simulated in LUARLW are exclusive in contrast to JETSET, where they are inclusive. In addition, LUARLW uses fewer free parameters in the fragmentation function than JETSET. Above 3.77 GeV, the production of charmed mesons is included in the generator according

to the Eichten Model [6,7].

The parameters in LUARLW are tuned to reproduce the observed multiplicity, sphericity, angular and momentum distributions, etc., over the entire energy region covered by the scan. We find that one set of parameter values is required for the cm energy region below open charm threshold, and that a second set is required for higher energies. In an alternative approach, the parameter values were tuned point-by-point throughout the entire energy range. We find that the detection efficiencies determined using individually tuned parameters are consistent with those determined with globally tuned parameters to within 2%. This difference is included in the systematic errors. The detection efficiencies were also determined using JETSET74 for the energies above 3 GeV. The difference between the JETSET74 and LUARLW results is about 1%, and is also taken into account in estimating the systematic uncertainty. Figure 2 shows the variation of the detection efficiency as a function of cm energy.

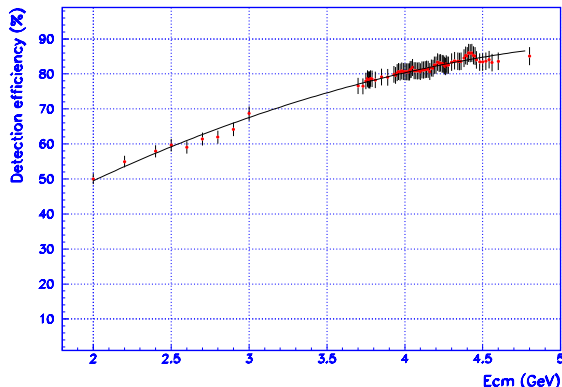


FIG. 2. The cm energy dependence of the detection efficiency for hadronic events estimated using the LUARLW generator.

Different schemes for the radiative corrections were compared [8–11]. As reported in Ref. 3, below charm threshold the four different schemes agree with each other to within 1%. Above charm threshold, where resonances are important, the agreement is within 1 to 3%. However, the schemes of Refs. 10 and 11 take into account vacuum polarization not only for electrons and muons, but also taus and hadrons. The correction factors calculated with these two approaches are consistent within 0.5% in the continuum and differ by less than 1% in the charm resonance region. The formalism of Ref. 11 is used in our calculation, and differences between it and the schemes described in Ref. 10 are included in the systematic errors. In the calculation of the radiative correction above charm threshold, where the resonances are broad and where the total width of the resonance is related to the energy, we take the interference between resonances into account.

Table II lists the R values measured by BES in this experiment. They are displayed in Fig. 3, together with BESII values from Ref.3 and those measured by MarkI,

$\gamma\gamma 2$, and Pluto [12–14]. The R values from BESII have an average uncertainty of about 6.6%, which represents a factor of two to three improvement in precision in the 2 to 5 GeV energy region. These improved measurements should have a significant impact on the global fit to the electroweak data and the determination of the SM prediction for the mass of the Higgs particle. In addition, they are expected to provide an improvement in the precision of the calculated value of a_μ^{SM} [15,16].

TABLE III. Error sources for $E_{cm}=3.0$ GeV. Adding the systematic and statistical errors in quadrature gives a total error of 5.8%.

Source	N_{had}	L	ϵ_{had}	$1 + \delta$	Stat.
Err.(%)	3.3	2.3	3.0	1.3	2.5

As a typical example, Table III lists the contributions to the uncertainty in the value of R at 3 GeV. Further improvements in the accuracy of R measurements at BEPC will require higher machine luminosity, especially for energies below 3.0 GeV, and better detector performance, particularly in the area of calorimetry. Increased precision in the areas of hadronic event simulation and the calculation of the radiative correction are also required.

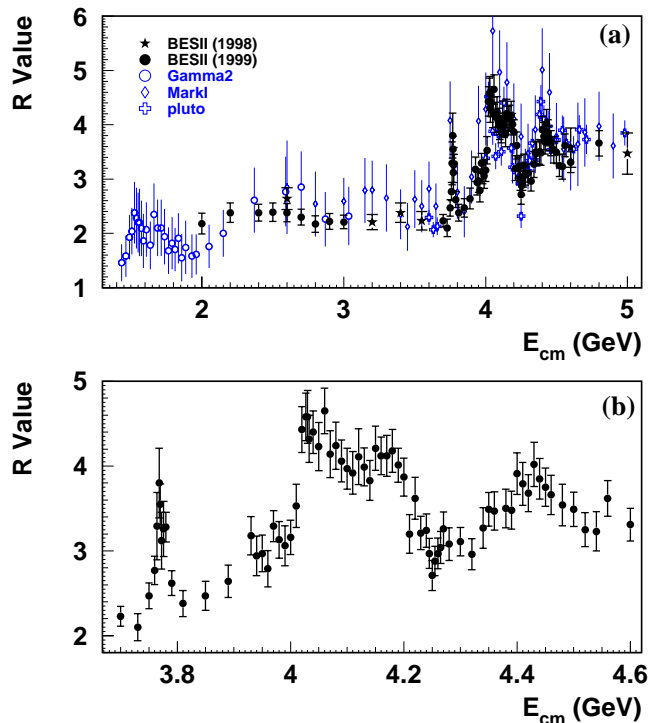


FIG. 3. (a) A compilation of measurements of R in the cm energy range from 1.4 to 5 GeV. (b) R values from this experiment in the resonance region between 3.75 and 4.6 GeV.

We would like to thank the staff of the BEPC Accelerator Center and IHEP Computing Center for their efforts.

TABLE II. The measured R values obtained in this experiment; the first error is statistical, the second systematic.

E_{cm} (GeV)	R	E_{cm} (GeV)	R	E_{cm} (GeV)	R	E_{cm} (GeV)	R	E_{cm} (GeV)	R
2.000	$2.18 \pm .07 \pm .18$	3.776	$3.26 \pm .26 \pm .19$	4.030	$4.58 \pm .20 \pm .23$	4.190	$4.01 \pm .14 \pm .14$	4.360	$3.47 \pm .13 \pm .18$
2.200	$2.38 \pm .07 \pm .17$	3.780	$3.28 \pm .12 \pm .12$	4.033	$4.32 \pm .17 \pm .22$	4.200	$3.87 \pm .16 \pm .16$	4.380	$3.50 \pm .15 \pm .17$
2.400	$2.38 \pm .07 \pm .14$	3.790	$2.62 \pm .11 \pm .10$	4.040	$4.40 \pm .17 \pm .19$	4.210	$3.20 \pm .16 \pm .17$	4.390	$3.48 \pm .16 \pm .16$
2.500	$2.39 \pm .08 \pm .15$	3.810	$2.38 \pm .10 \pm .12$	4.050	$4.23 \pm .17 \pm .22$	4.220	$3.62 \pm .15 \pm .20$	4.400	$3.91 \pm .16 \pm .19$
2.600	$2.38 \pm .06 \pm .15$	3.850	$2.47 \pm .11 \pm .13$	4.060	$4.65 \pm .19 \pm .19$	4.230	$3.21 \pm .13 \pm .15$	4.410	$3.79 \pm .15 \pm .20$
2.700	$2.30 \pm .07 \pm .13$	3.890	$2.64 \pm .11 \pm .15$	4.070	$4.14 \pm .20 \pm .19$	4.240	$3.24 \pm .12 \pm .15$	4.420	$3.68 \pm .14 \pm .17$
2.800	$2.17 \pm .06 \pm .14$	3.930	$3.18 \pm .14 \pm .17$	4.080	$4.24 \pm .21 \pm .18$	4.245	$2.97 \pm .11 \pm .14$	4.430	$4.02 \pm .16 \pm .20$
2.900	$2.22 \pm .07 \pm .13$	3.940	$2.94 \pm .13 \pm .19$	4.090	$4.06 \pm .17 \pm .18$	4.250	$2.71 \pm .12 \pm .13$	4.440	$3.85 \pm .17 \pm .17$
3.000	$2.21 \pm .05 \pm .11$	3.950	$2.97 \pm .13 \pm .17$	4.100	$3.97 \pm .16 \pm .18$	4.255	$2.88 \pm .11 \pm .14$	4.450	$3.75 \pm .15 \pm .17$
3.700	$2.23 \pm .08 \pm .08$	3.960	$2.79 \pm .12 \pm .17$	4.110	$3.92 \pm .16 \pm .19$	4.260	$2.97 \pm .11 \pm .14$	4.460	$3.66 \pm .17 \pm .16$
3.730	$2.10 \pm .08 \pm .14$	3.970	$3.29 \pm .13 \pm .13$	4.120	$4.11 \pm .24 \pm .23$	4.265	$3.04 \pm .13 \pm .14$	4.480	$3.54 \pm .17 \pm .18$
3.750	$2.47 \pm .09 \pm .12$	3.980	$3.13 \pm .14 \pm .16$	4.130	$3.99 \pm .15 \pm .17$	4.270	$3.26 \pm .12 \pm .16$	4.500	$3.49 \pm .14 \pm .15$
3.760	$2.77 \pm .11 \pm .13$	3.990	$3.06 \pm .15 \pm .18$	4.140	$3.83 \pm .15 \pm .18$	4.280	$3.08 \pm .12 \pm .15$	4.520	$3.25 \pm .13 \pm .15$
3.764	$3.29 \pm .27 \pm .29$	4.000	$3.16 \pm .14 \pm .15$	4.150	$4.21 \pm .18 \pm .19$	4.300	$3.11 \pm .12 \pm .12$	4.540	$3.23 \pm .14 \pm .18$
3.768	$3.80 \pm .33 \pm .25$	4.010	$3.53 \pm .16 \pm .20$	4.160	$4.12 \pm .15 \pm .16$	4.320	$2.96 \pm .12 \pm .14$	4.560	$3.62 \pm .13 \pm .16$
3.770	$3.55 \pm .14 \pm .19$	4.020	$4.43 \pm .16 \pm .21$	4.170	$4.12 \pm .15 \pm .19$	4.340	$3.27 \pm .15 \pm .18$	4.600	$3.31 \pm .11 \pm .16$
3.772	$3.12 \pm .24 \pm .23$	4.027	$4.58 \pm .18 \pm .21$	4.180	$4.18 \pm .17 \pm .18$	4.350	$3.49 \pm .14 \pm .14$	4.800	$3.66 \pm .14 \pm .19$

We thank B. Andersson for helping in the development of the LUARLW generator. We also wish to acknowledge useful discussions with M. Davier, B. Pietrzyk, T. Sjöstrand, A. D. Martin and M. L. Swartz. We especially thank M. Tigner for major contributions not only to BES but also to the operation of the BEPC during the R scan.

This work is supported in part by the National Natural Science Foundation of China under Contract Nos. 19991480, 19805009 and 19825116; the Chinese Academy of Sciences under contract Nos. KJ95T-03, and E-01 (IHEP); and by the Department of Energy under Contract Nos. DE-FG03-93ER40788 (Colorado State University), DE-AC03-76SF00515 (SLAC), DE-FG03-94ER40833 (U Hawaii), DE-FG03-95ER40925 (UT Dallas), and by the Ministry of Science and Technology of Korea under Contract KISTEP I-03-037(Korea).

(1981).

- [9] G. Bonneau and F. Martin, *Nucl. Phys. B* **27**, 387 (1971).
- [10] E. A. Kuraev and V.S. Fadin, *Sov. J. Nucl. Phys.* **41**, 3(1985).
- [11] C. Edwards *et al.*, SLAC-PUB-5160, 1990. (T/E)
- [12] J. L. Siegrist *et al.*, (Mark I Collab.), *Phys. Lett. B* **26**, 969 (1982).
- [13] C. Bacci *et al.*, ($\gamma\gamma 2$ Collab.), *Phys. Lett. B* **86**, 234 (1979).
- [14] L. Criegee and G. Knies, (Pluto Collab.), *Phys. Rep.* **83**, 151 (1982);
Ch. Berger *et al.*, *Phys. Lett. B* **81**, 410 (1979).
- [15] B. Pietrzyk, Robert Carey, Atul Gurtu, talks given at ICHEP2000, Osaka, Japan, July 2000.
- [16] A. Martin *et al.*, *Phys. Lett. B* **492**, 69 (2000).

- [1] Z.G. Zhao, International Journal of Modern Physics A15 (2000)3739.
- [2] J.Z. Bai *et al.*, (BES Collab.), *Nucl. Instrum. Methods* **458**, 627 (2001).
- [3] J. Z. Bai *et al.*, (BES Collab.), *Phys. Rev. Lett.* **84**, 594 (2000).
- [4] Z.G. Zhao, *Nucl. Phys. A* **675**, 13c (2000).
- [5] B. Andersson and Haiming Hu, "Few-body States in Lund String Fragmentation Model" hep-ph/9910285.
- [6] E. Eichten *et al.*, *Phys. Rev. D* **21**, 203 (1980).
- [7] J.C. Chen *et al.*, *Phys. Rev. D* **62**, 034003 (2000).
- [8] F.A. Berends and R. Kleiss, *Nucl. Phys. B* **178**, 141